SAND2018-2829C

Properties of Brines Formed by Deliquescence of Sea-Salt Aerosols

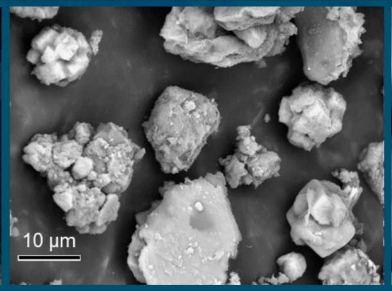

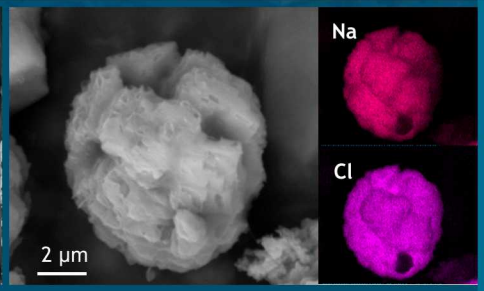

PRESENTED BY

Charles Bryan and Eric Schindelholz

Sandia National Laboratories is a multimission laboratory managed and operated by National Technology and Engineering Solutions of Sandia LLC, a wholly owned subsidiary of Honeywell International Inc. for the U.S. Department of Energy's National Nuclear Security Administration under contract DE-NA0003525. SAND2018-xxxxxx

Overview

- Context: Atmospheric corrosion of metals
  - Extent of damage: dependence on brine layer properties (e.g., Chen and Kelly, 2010 model).
  - Specific application corrosion of in-service spent nuclear fuel (SNF) interim storage canisters
- Brine properties as a function of relative humidity (RH) and temperature
  - Thermodynamic modeling (equilibrium modeling)
  - Experimental measurements
- Possible effects of particle-gas conversion reactions not considered in the modeling
- Conclusions

Atmospheric corrosion

Pitting corrosion:

- Metal oxidation occurs in the pit (anode), while the oxygen reduction (cathodic reaction) occurs on the surrounding surface.
- Cathode and anode must be connected by a conductive aqueous film: anode current demand must be met by cathode current
- Maximum possible anode current (maximum pit size) is determined by the maximum available cathode current (Chen and Kelly 2010).
- Maximum cathode current is function of brine layer *conductivity* and *thickness*, in turn functions of *temperature*, *RH*, and *salt load.*

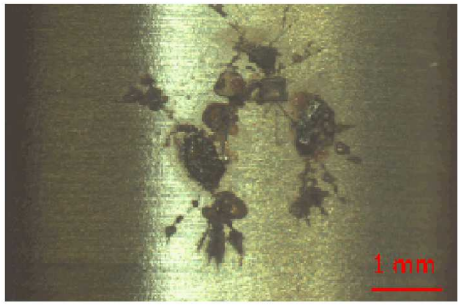

Maximum Pit Size

(Chen and Kelly 2010)

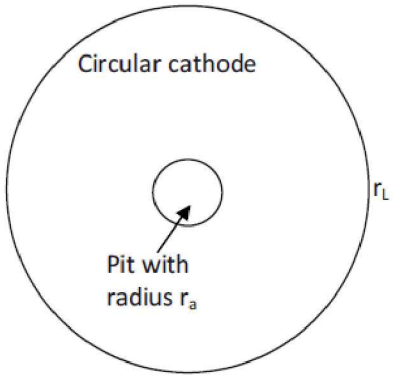

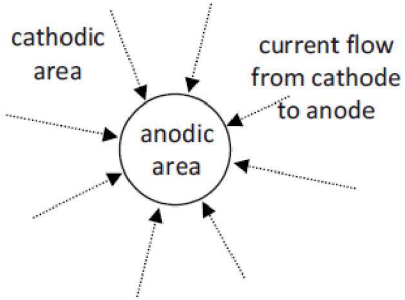

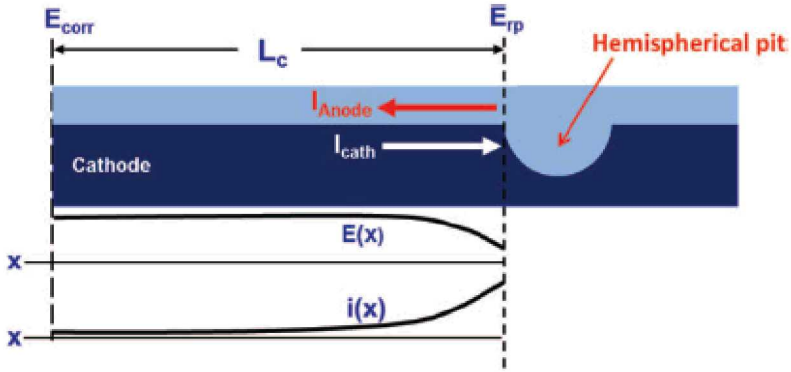

Chen et al., 2008

Max. cathode current — Brine conductivity — Brine layer thickness — Cathodic kinetics

$$\ln I_{c,max} = \frac{4\pi k W_L \Delta E_{max}}{I_{c,max}} + \ln\left[\frac{\pi e r_a^2 \int_{E_{corr}}^{E_{rp}} (I_c - I_p) dE}{\Delta E_{max}}\right]$$

Specific Application: Corrosion of SNF Interim Storage Canisters

Horizontal storage systems

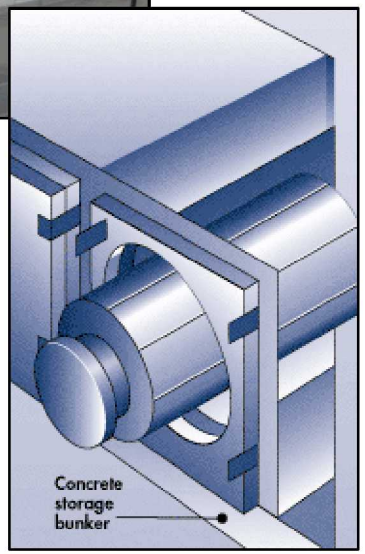

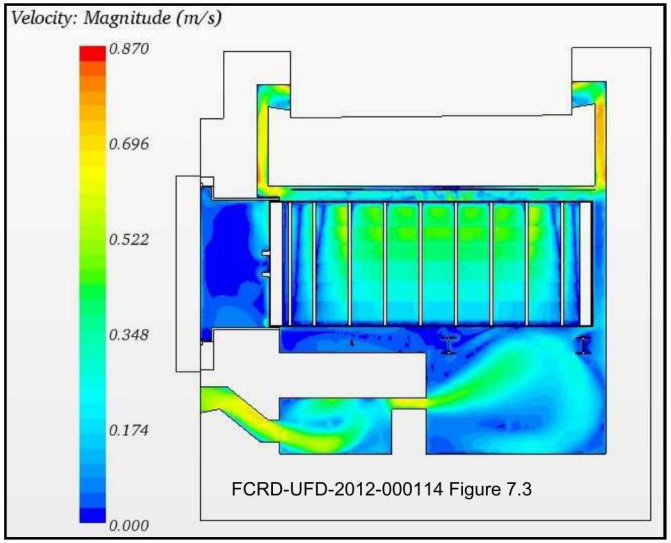

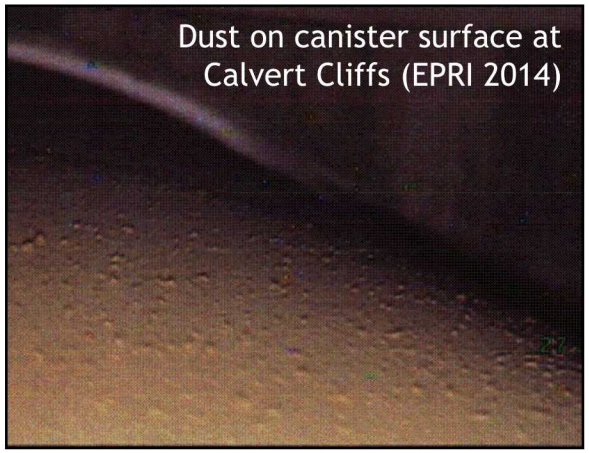

<u>Stainless steel canisters within concrete/steel overpacks</u>

- Horizontal or vertical orientation
- Passively ventilated
- Over time, dust aerosols accumulate on the canister surface

Dust compositions: Sea-salt aerosols deposited at some near-marine storage sites

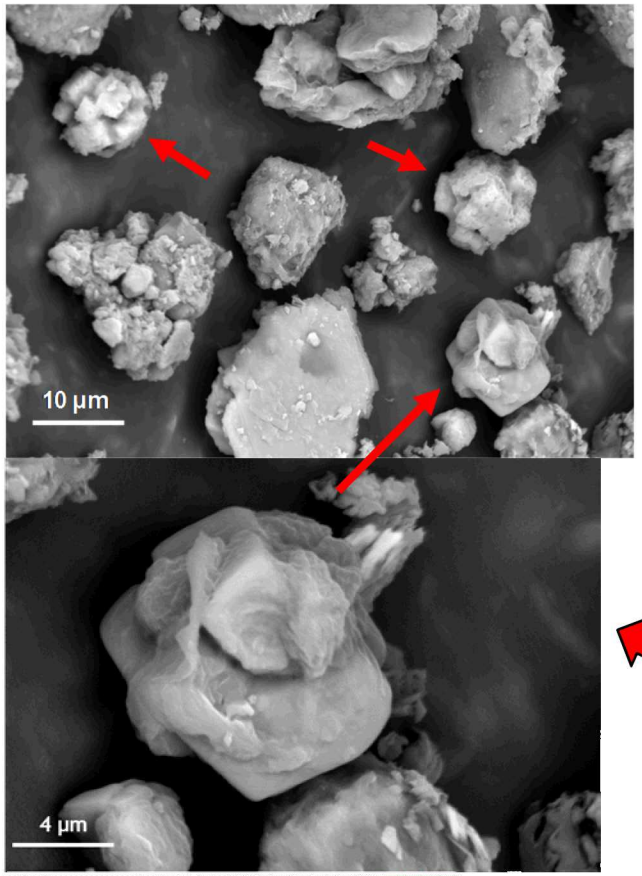

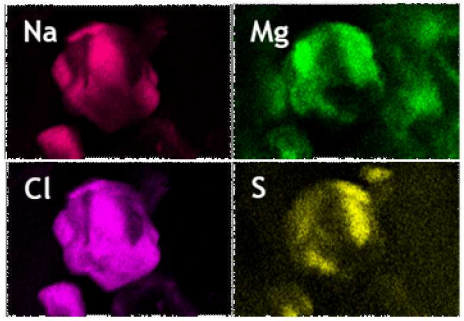

At some near-marine ISFSI sites, sea-salt aerosols are deposited on canister surfaces

:es in
n

Diablo
SFSI

Locations of U.S. Spent Nuclear Fuel Independent Storage Installations

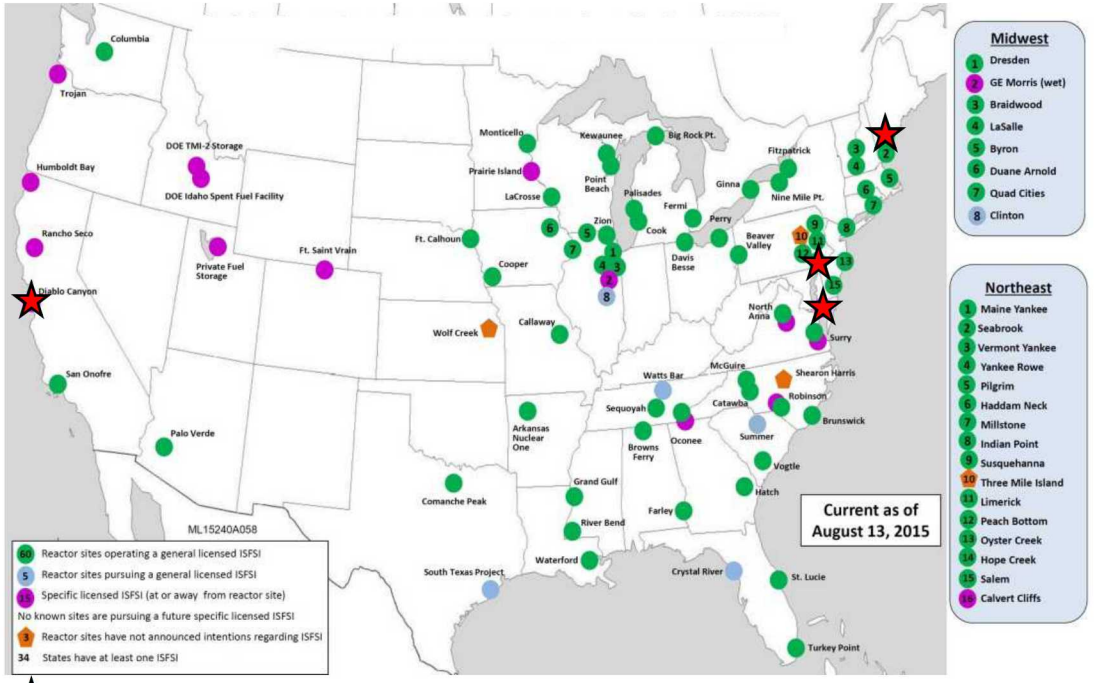

★ Locations where dust and soluble salt samples have been collected

Evolution of Canister Surface Environment

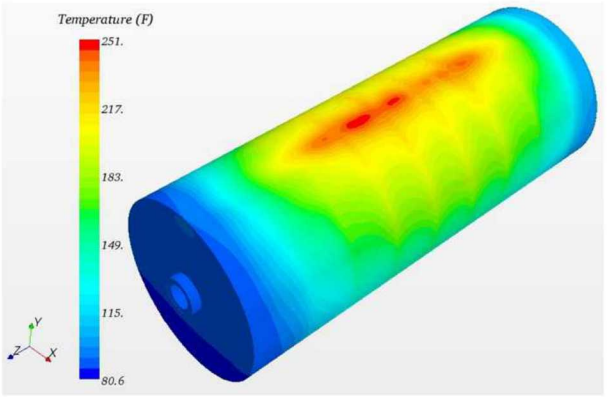

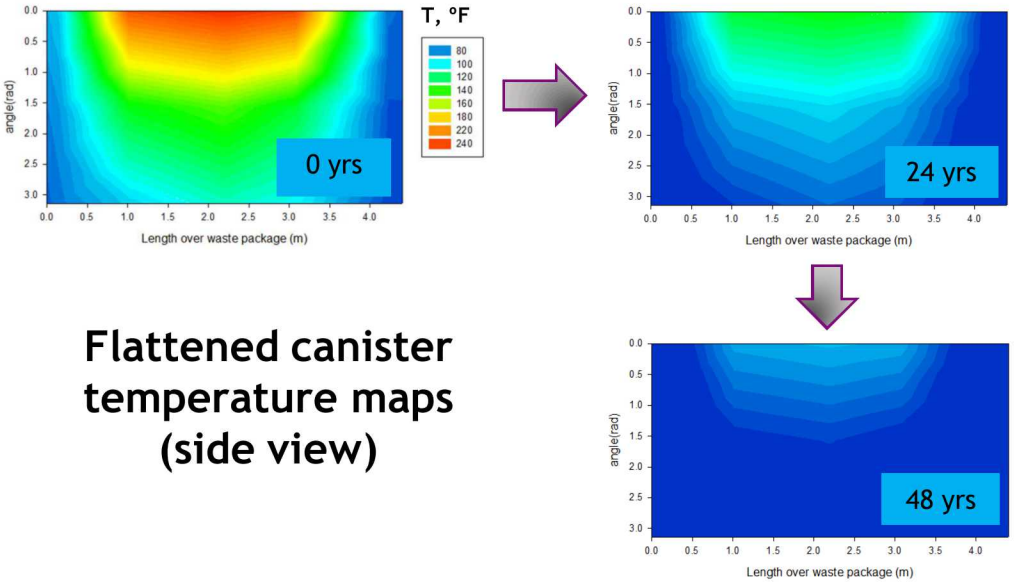

Flattened canister temperature maps (side view)

Over time, during storage:

- Canister dust load increases
- Canister cools
  - Salts eventually deliquesce, forming surface brines
  - Brine layer properties change as salt load and RH continue to increase

Evaluate brine layer properties as a function of T, RH, and salt load

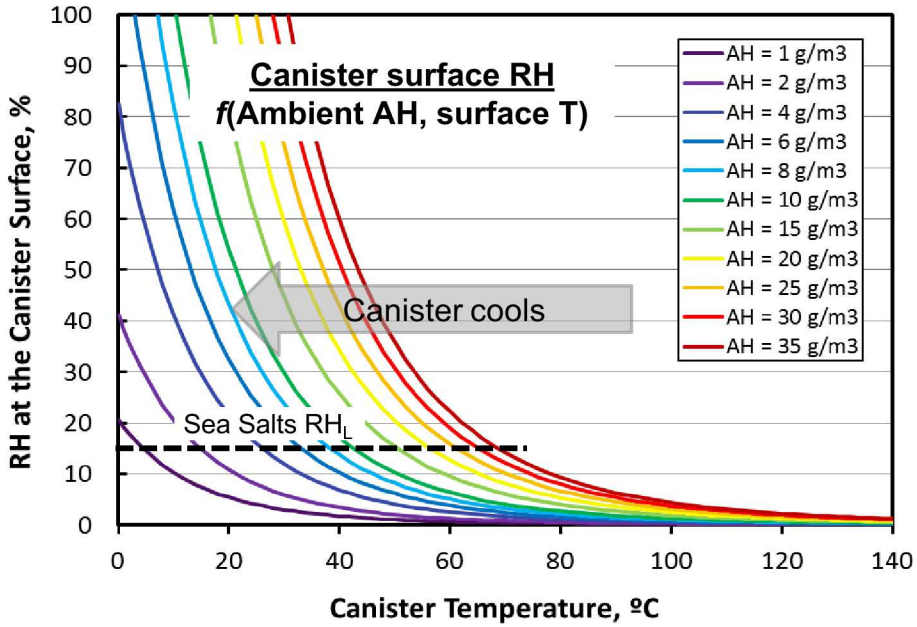

Thermodynamic modeling of brines formed by sea-salt deliquescence

Thermodynamic modeling:

- Carried out using geochemical speciation and solubility code EQ3/6 (Wolery and Jarek, 2003).
- Modeled as seawater evaporation: evaporation is the reverse of deliquescence, predicts the same brine compositions as a function of RH
- Starting seawater composition taken as that of ASTM D 1141-98.
- Assumes equilibrium with atmospheric CO_2 concentration of $10^{-3.4}$ bars, but does not limit or constrain acid gas concentrations. Does not consider other atmospheric exchange reactions.

Sea salt/spray — generally simulated with synthetic ocean water *(ASTM D1141-98)*

	Conc., mg/L	
Species	**ASTM D1141-98**	**McCaffrey et al. (1987)**
Na^+	11031	11731
K^+	398	436
Mg^{2+}	1328	1323
Ca^{2+}	419	405
Cl^-	19835	21176
Br^-	68	74
F^-	1	—
SO_4^{2-}	2766	2942
BO_3^{3-}	26	—
HCO_3^-	146	—
pH	8.2	8.2

Thermodynamic Database

- Thermodynamic database:
  - *data0.ypf.R2*, developed for the Yucca Mountain Program (SNL 2007)
  - Implements Pitzer model for activity coefficients in high ionic strength solutions (Pitzer, 1991)
  - Completely consistent –experimental data for all species refitted to a consistent set of aqueous species and Pitzer parameters.
  - Database based on thermodynamic model of Harvie, Eugster, and coworkers, 1980a,b; 1984) for natural waters, with many added salts.
  - For sea-salts, based on experimental work by Van't Hoff (1905, 1909, 1912) at temperatures up to 80ºC, and with added data from many other researchers.
  - Thoroughly validated for aqueous solutions of individual salts and salt mixtures, including brines formed by seawater evaporation. Validated to 140ºC.
  - Consistent with several experimental studies of seawater evaporation dating back to the mid-1800s, and with observed salt assemblages in geologic evaporate deposits.

Thermodynamic model validation
(example of seawater evaporation)

Model validation against seawater evaporation data from the Morton salt facility at Inagua Island, Bahamas

(data from McCaffrey et al., 1987)

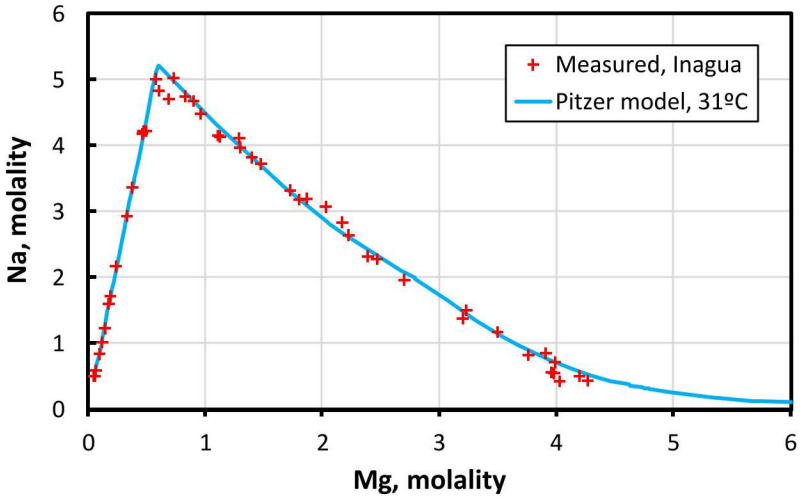

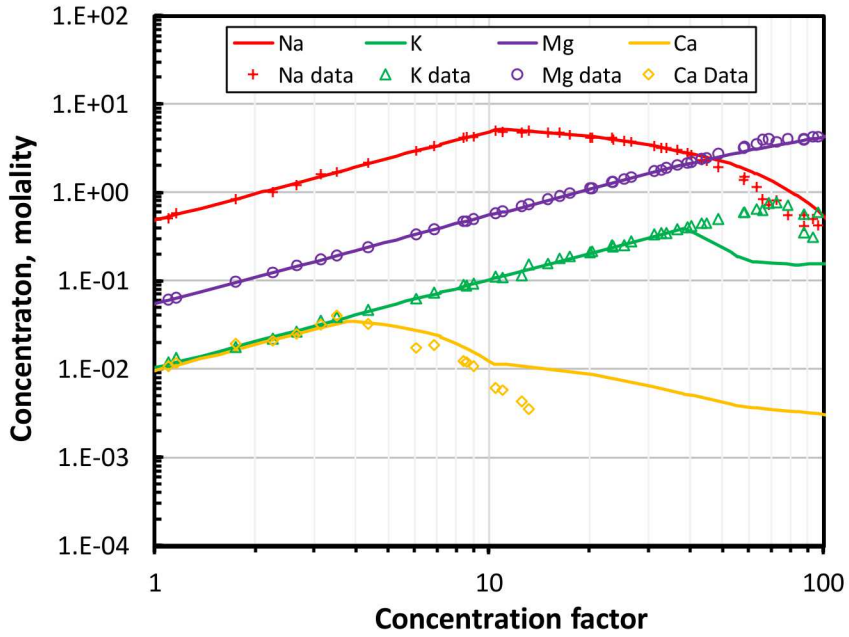

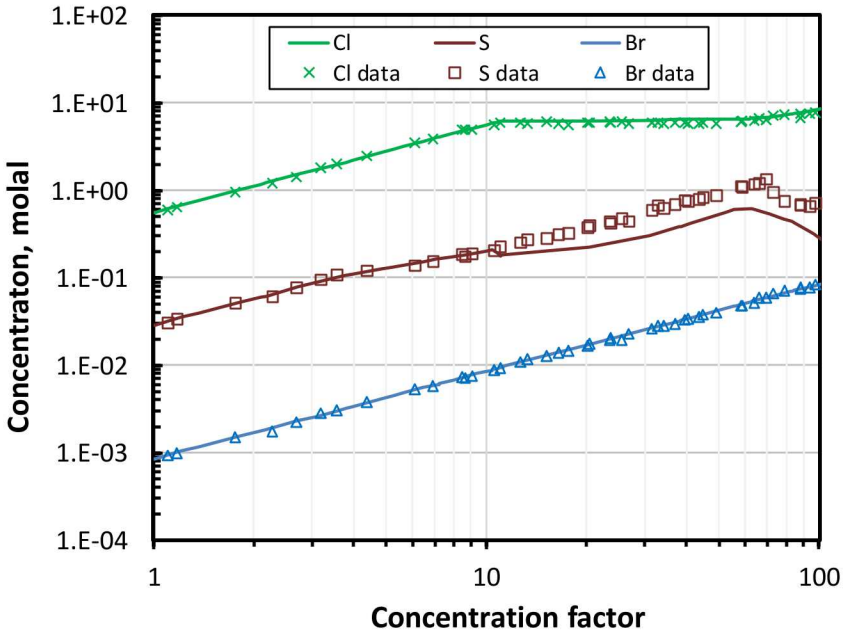

Sea-salt Deliquescent Brine Compositions

Seawater evaporation/deliquescence at 25ºC

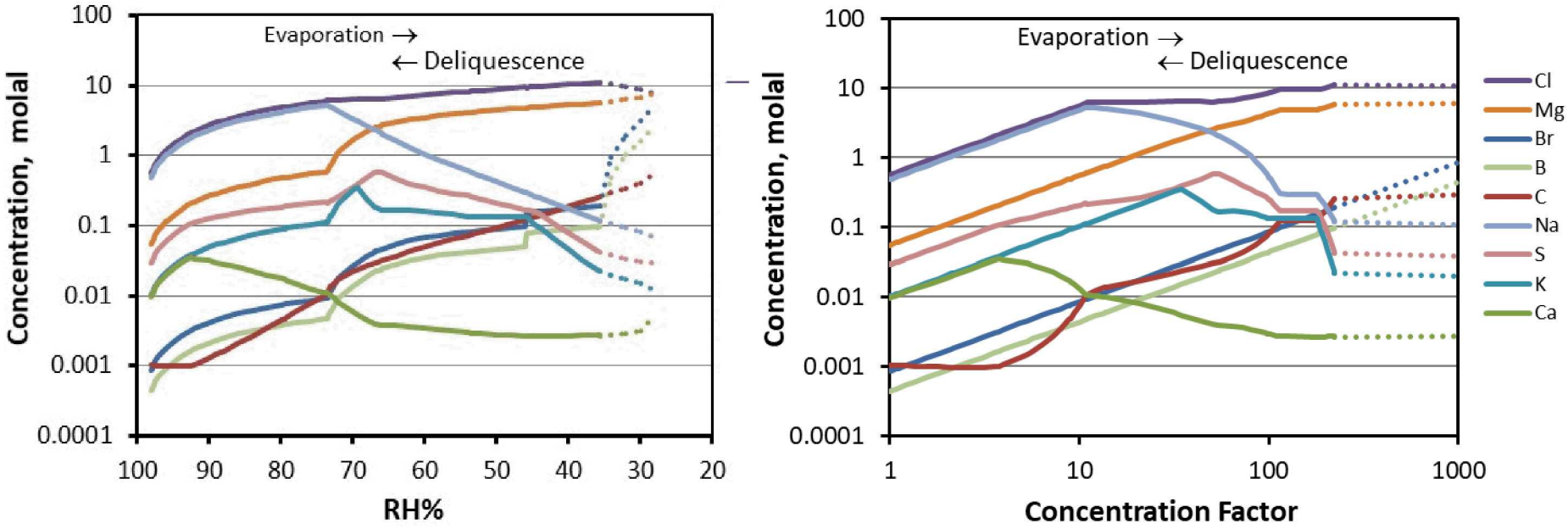

Brine compositions:

- *Upon evaporation, salts precipitate and redissolve. Predipitated salts dictate the composition of remaining brine*
- *Seawater evolves towards concentrated Mg-Cl brine as NaCl precipitates*
- *Ca, K, S are mostly removed by minerals, and are very low in the final remaining brine*
- *Br and B are conserved (but the thermodynamic database is not qualified for B compounds)*
- *General trends vary little with temperature (10-80ºC)*

Seawater Evaporation: Precipitated Salts

Precipitated salts:

Upon evaporation, several salts precipitate and re-dissolve (order given below). The final assemblage determines the deliquescence RH.

Final assemblage
- NaCl (halite)
- $MgCl_2:6H_2O$ (bischofite)
- $MgSO_4:2H_2O$ (kieserite)
- $KMgCl_3:6H_2O$ (carnallite)
- $CaSO_4$ (anhydrite)
- $Mg_5(CO_3)_4(OH)_2:4H_2O$ (hydromagnesite)

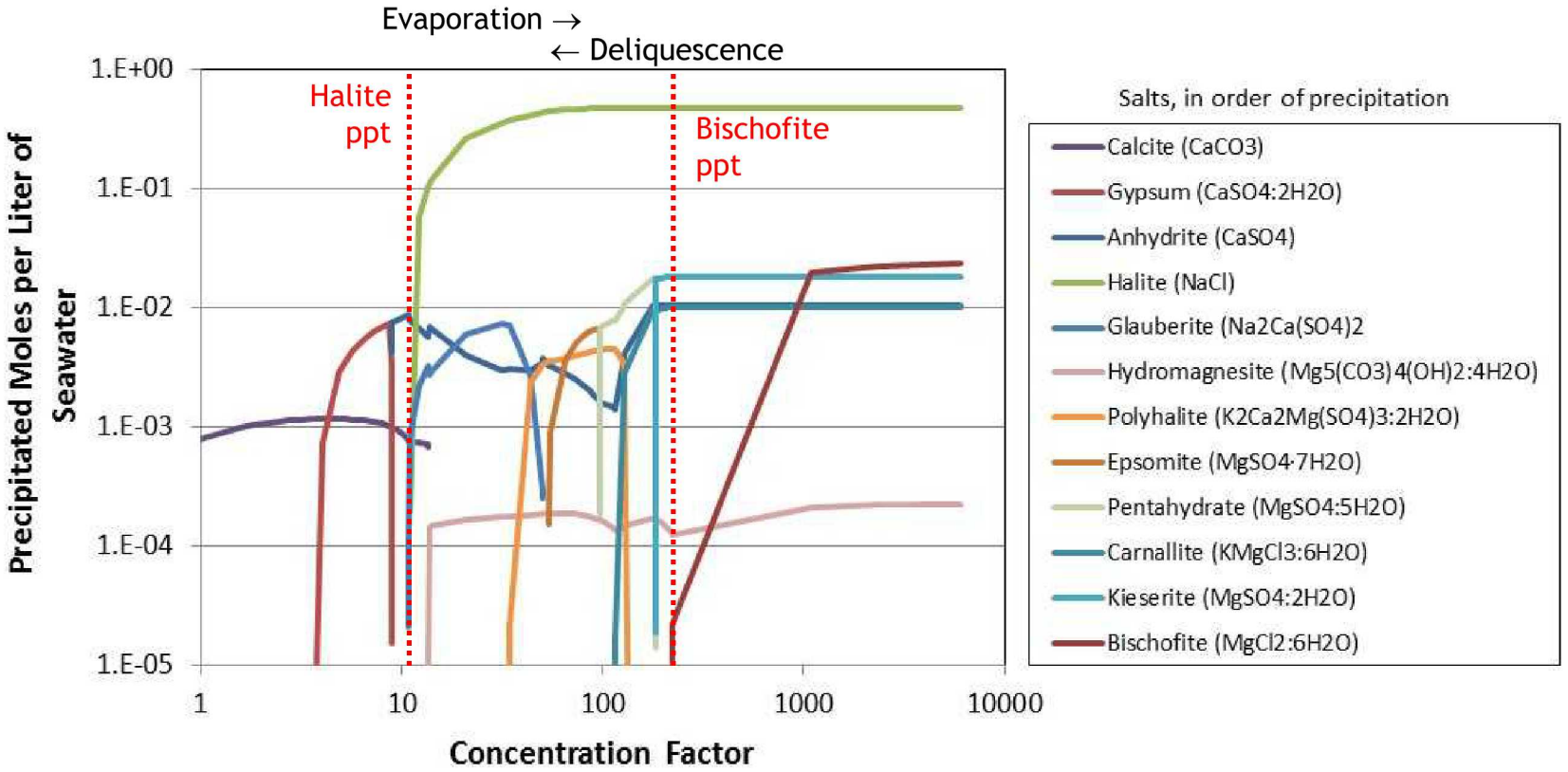

Sea-salt Deliquescent Brine Compositions

Predicted O_2 solubilities in sea-salt brines

- Implemented in Pitzer database based on data from Clegg and Brimblecombe (1990)
- *Not validated against independent data*

Important parameter for corrosion, as it affects the kinetics of the oxygen reduction reaction (ORR) at the cathode.

O_2 solubility predicted to decrease with:

- increasing ionic strength
- increasing temperature at >74% RH (in Na-rich brines); but at <74% RH (Mg-rich brines), the trend is reversed.

If accurate, we postulate:

- Under conditions when oxygen diffusion is the rate limiting step for ORR, cathode kinetics will be reduced in concentrated brines
- In concentrated brines, films must be thinner before oxygen diffusion is no longer rate limiting.

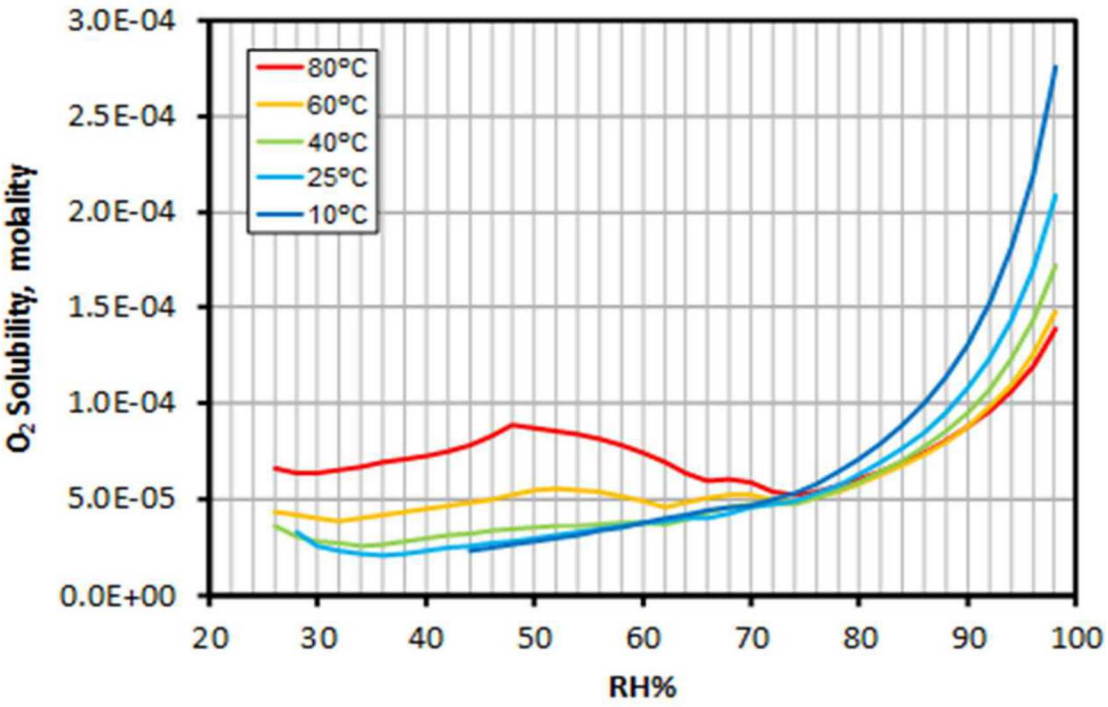

Brines Selected for Experimental Measurement of Brine Properties

Selected brine compositions mixed to measure brine properties as a function of RH, T:

- Density – Required to calculate brine volumes (brine layer thicknesses)
- Conductivity
- Cathodic polarization curves (not presented here)

Brines based on model estimates of compositions at:

- Unevaporated Seawater (98% RH)
- Evap. to 78% RH
- Evap. to 56% RH
- Evap. to 38% RH

Use of 25ºC brine compositions to estimate brine properties at elevated temperature introduces some error for low RH brines, where the ionic strength vary as much as ~10% with temperature.

Composition of Brines Used for Experimental Testing

Brine RH	Species Concentration (molality)									
	Na^+	K^+	Mg^{2+}	Ca^{2+}	Cl^-	Br^-	F^-	SO_4^{2-}	BO_3^{3-}	HCO_3^-
98% (SW)	0.498	0.011	0.057	0.011	0.580	0.001	0.0001	0.030	0.001	0.002
78%	4.507	0.096	0.513	0.015	5.250	0.008	—	0.196	0.004	0.006
56%	0.719	0.144	3.907	0.003	7.941	0.077	—	0.289	0.040	0.064
38%	0.145	0.032	5.500	0.003	10.610	0.181	—	0.059	0.093	0.215

Measured Brine Densities

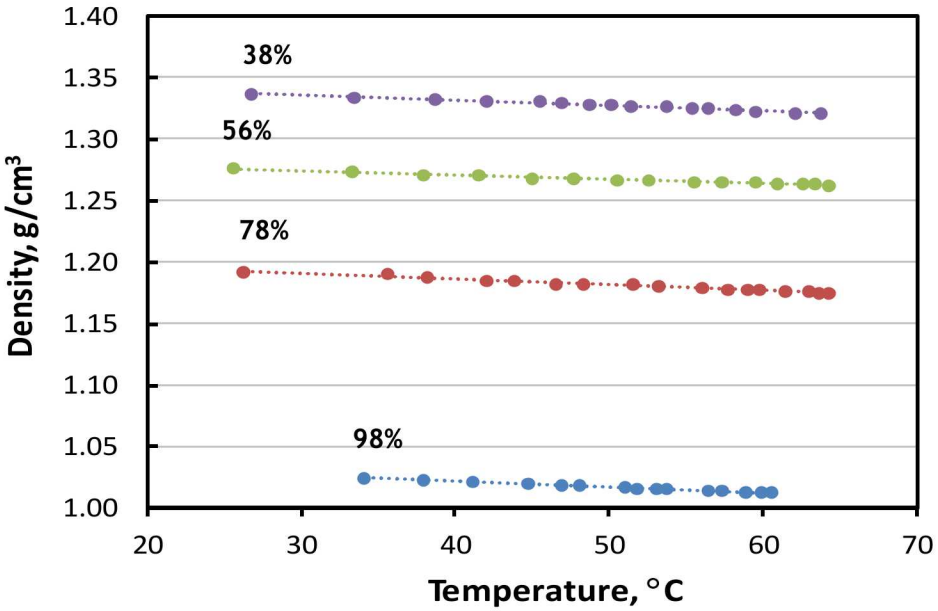

Brine specific gravities (specific gravities differ from density by <0.01%) measured using hydrometers

- *Calibration at elevated temperatures verified by measuring saturated NaCl solutions of known density*
- *Densities vary linearly with temperature, allowing simple extrapolation beyond the measured range.*

Comparison of measured density data with Inagua field data from McCaffrey et al. (1987)

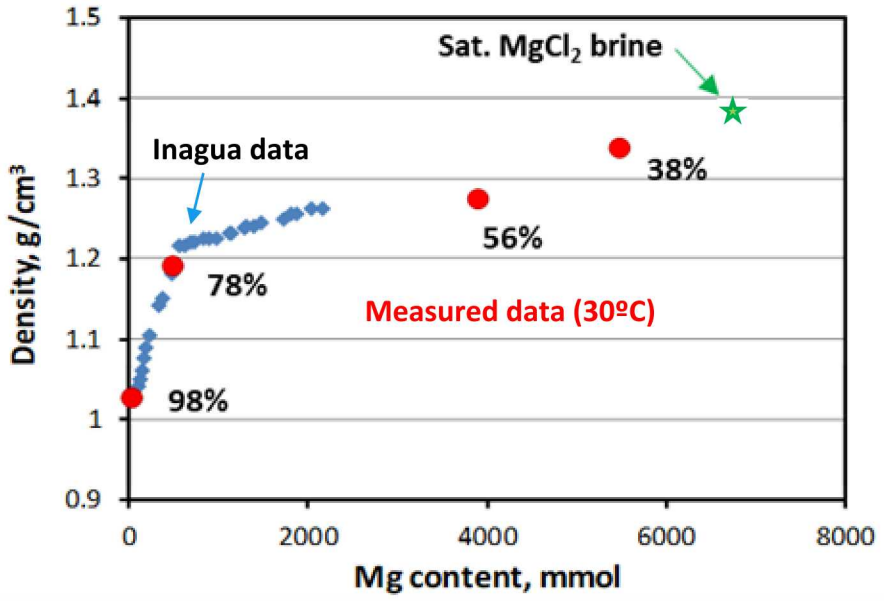

Brine Layer Thicknesses

Brine volumes based on geochemical modeling (mass of water/solutes remaining) and measured brine density data. Brine is assumed to be uniformly distributed on surface.

- Brine layer thicknesses decrease by orders of magnitude as brines evaporate and salts precipitate
- For any given RH, temperature has little effect on brine volume
  - Slight shift due to changes in RH of precipitation of ternary salts at 50% RH
  - Change in RH at which bischofite precipitates
- Volume varies linearly with salt load

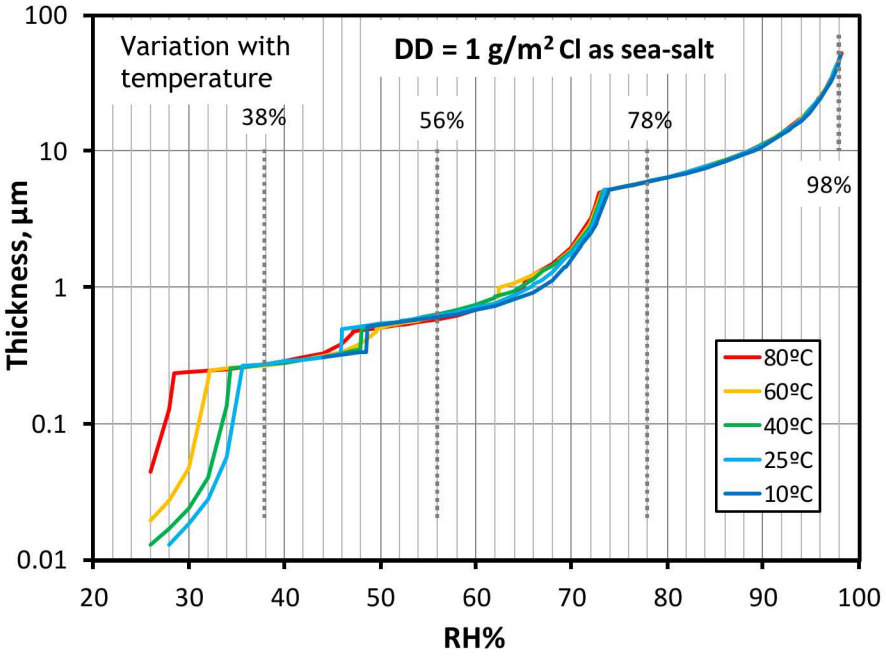

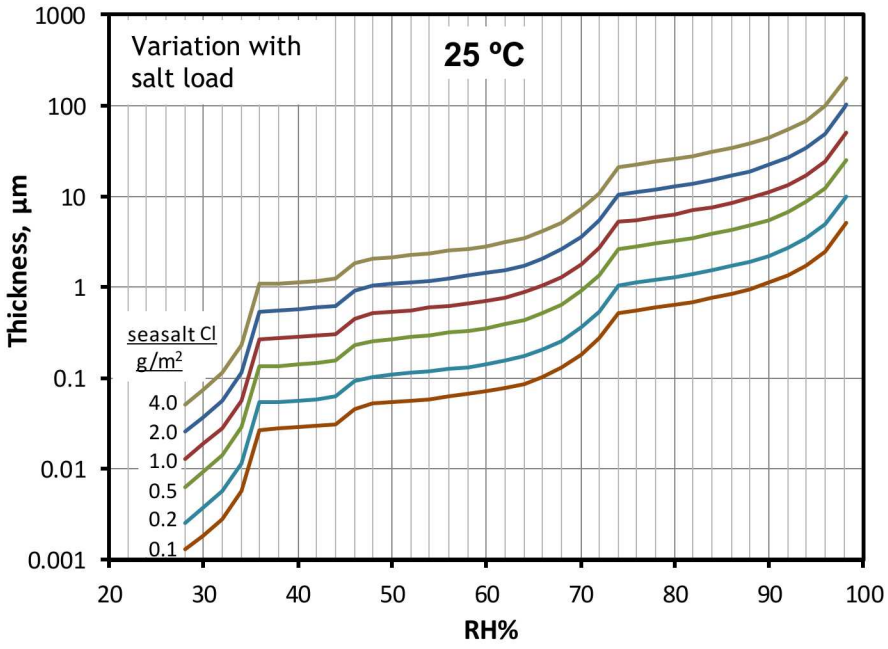

Brine Layer Properties

Sea-salt brines: ratio of brine volume to salt volume

Brine volume decreases rapidly with evaporation, while salts accumulate.

- Once NaCl precipitates (74% RH), brine/solid ratio drops rapidly.
- Below 60% RH, salt volume exceeds brine volume.
- Below 45%, brine volume is 0.3-0.4 of salt volume.
- At point of bischofite precipitation (deliquescence) brine volume is 0.3 salt volume.

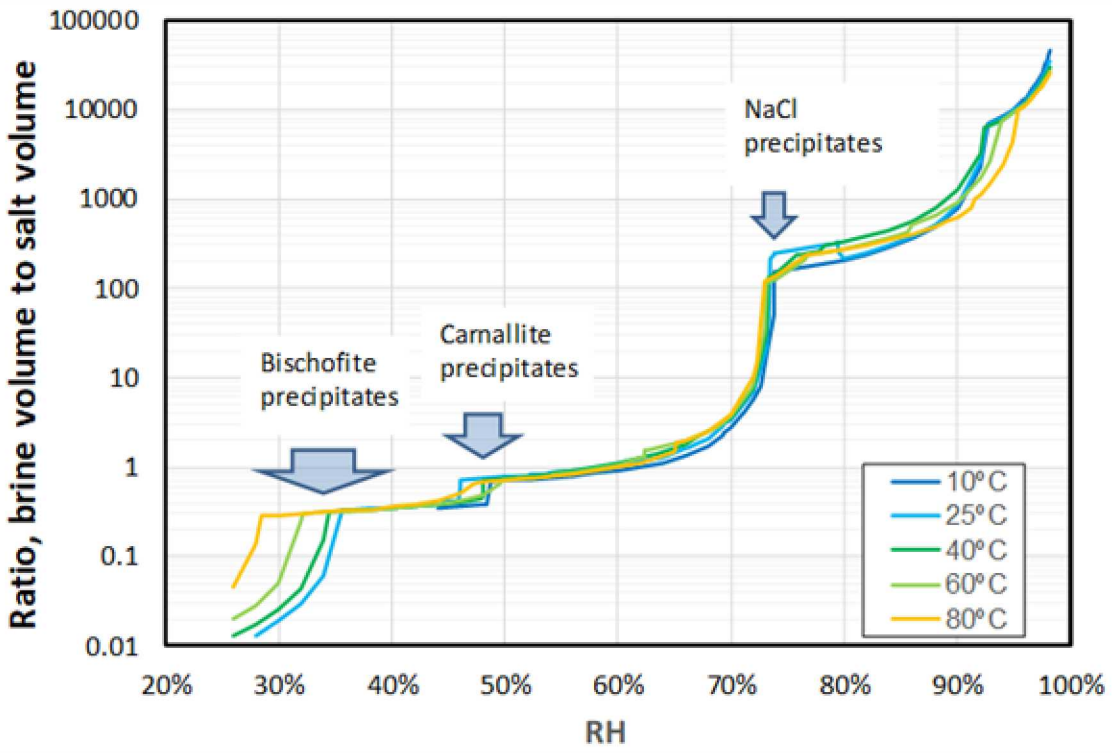

For sea-salts deposited as discrete salt aerosols, the assumption that brine forms a continuous layer may be unlikely, at low salt loads or low RH values. *However:*

- Experimental data suggest that the cathode can extend well beyond the perimeter of salt grains (Schindelholz et al., 2016).
- Insoluble dust particles will increase brine film continuity via capillary effects.

Brine Conductivity

- Conductivities vary linearly with temperature, allowing extrapolation beyond the measured range.
- Conductivity increases with Na concentration up to 74% RH (~6 molal NaCl)
- At lower RH, conductivity decreases as Mg increases. Consistent with anticipated behavior of divalent cation-rich brines, due to ion pair formation (Bockris and Reddy, 2002).

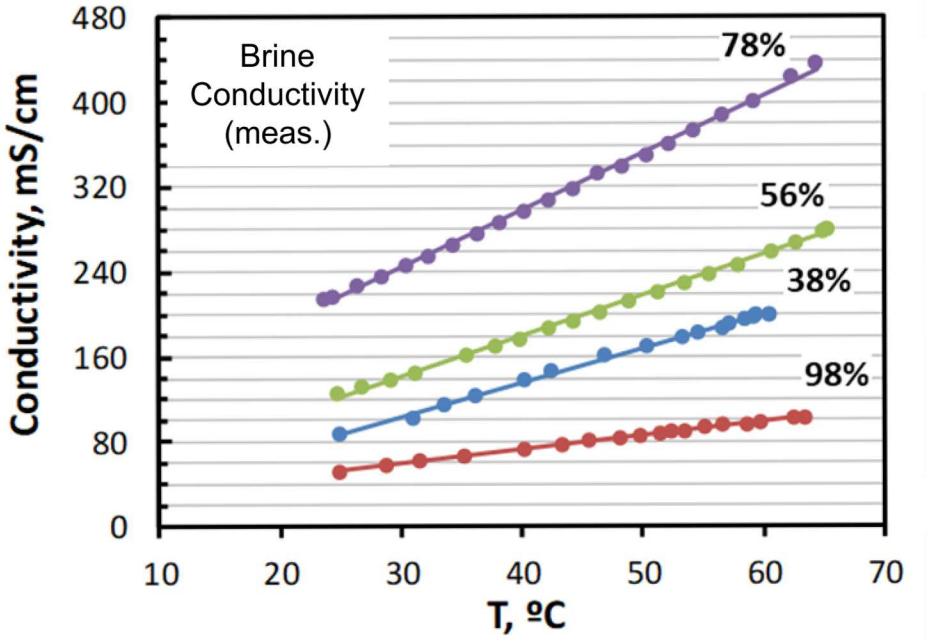

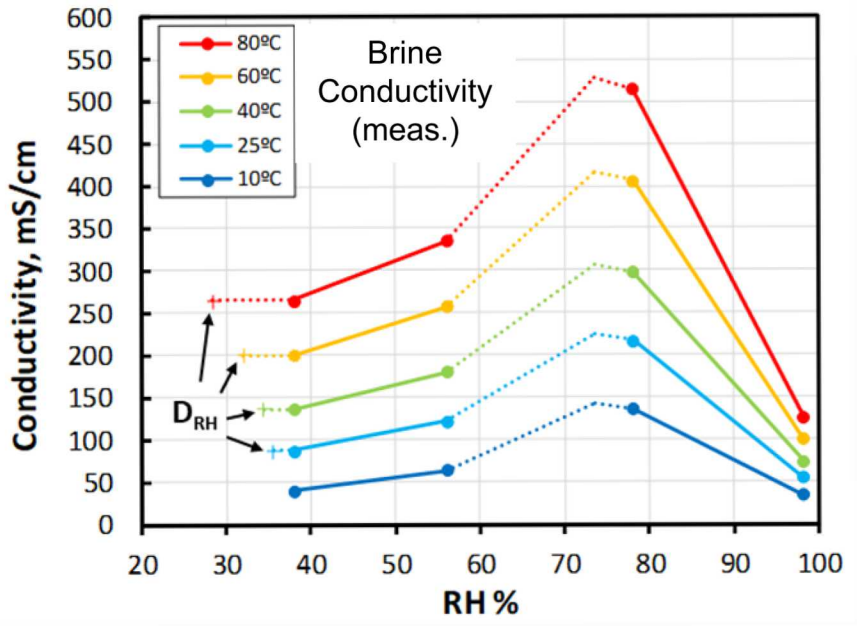

Combining Brine Layer Thickness and Conductivity

- Combining brine layer thickness and conductivity yields ~conductance.
  - High salt loads at low RH and low salt loads at high RH may result in similar brine conductances and extent of corrosion.
  - Controlling these parameters independently is important in experimental testing.

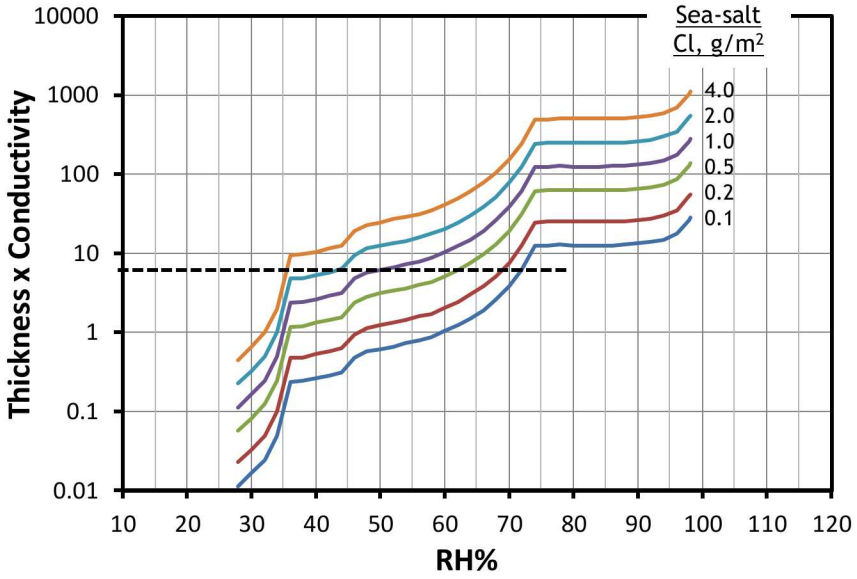

- Magnesium chloride is a poor analog for sea-salts in corrosion experiments—for a given chloride load, the brine volume is much higher
  - Only a small fraction of total sea-salt chlorides deliquesce to form magnesium chloride brine.

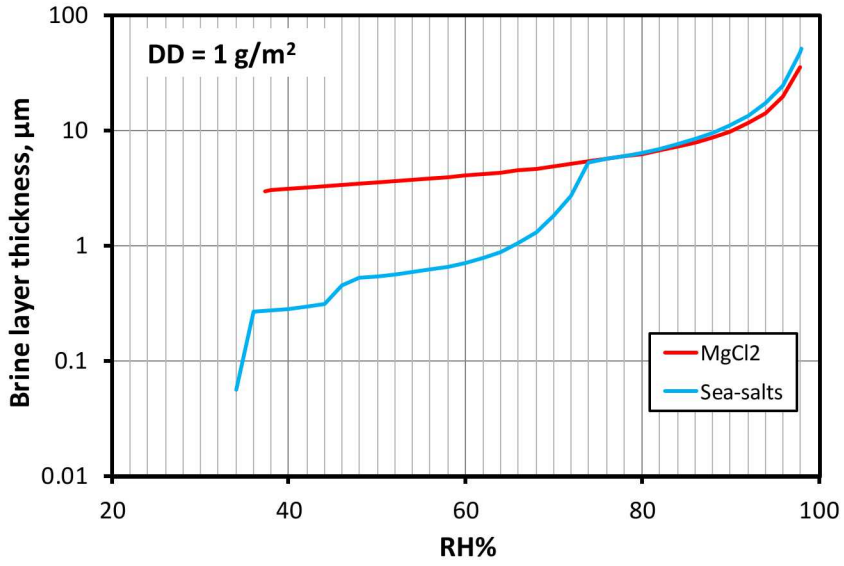

Effect of Atmospheric Exchange Reactions

Thermodynamic modeling results do not consider possible chloride loss through reactions with atmospheric gases. Very important for aerosol particles.

- Absorption of CO_2 and acid gas (H_2SO_4, HNO_3) resulting in HCl degassing:

$$NaCl(s, aq) + HNO_3(g) \leftrightarrow NaNO_3(s, aq) + HCl(g)$$

$$2NaCl(s, aq) + H_2O + \tfrac{1}{2}O_2 + SO_2(g) \leftrightarrow Na_2SO_4(s) + 2HCl(g)$$

And similar reactions that occur with Ca, Mg. For instance:

$$Mg^{+2}(aq) + 2Cl^{-}(aq) + H_2O + CO_2(g) \rightarrow MgCO_3(s) + 2HCl(g)$$

We are currently evaluating the last reaction, which is strongly temperature-dependent.

- Once corrosion initiates, effects of cathodic reactions on surface brine compositions (hydroxide generation, carbonation). We are also evaluating these reactions.

Stability of $MgCl_2$ Brines (Carbonation)

$$Mg^{2+} + 2Cl^- + CO_2(g) + H_2O \leftrightarrow MgCO_3(s) + 2HCl(g)$$

- Carbonation would result in brine dryout, eliminating corrosive environment.
- HCl gas partial pressures generated by Mg-Cl brines are strongly temperature-dependent. Higher temperatures result in higher HCl partial pressures.
- $MgCl_2$ brine stability is a function of temperature and background atmospheric HCl concentration; brine may absorb CO_2 and convert to Mg-carbonate at high temperatures.
- For SNF storage canisters, reaction could reverse itself as the canister cools.

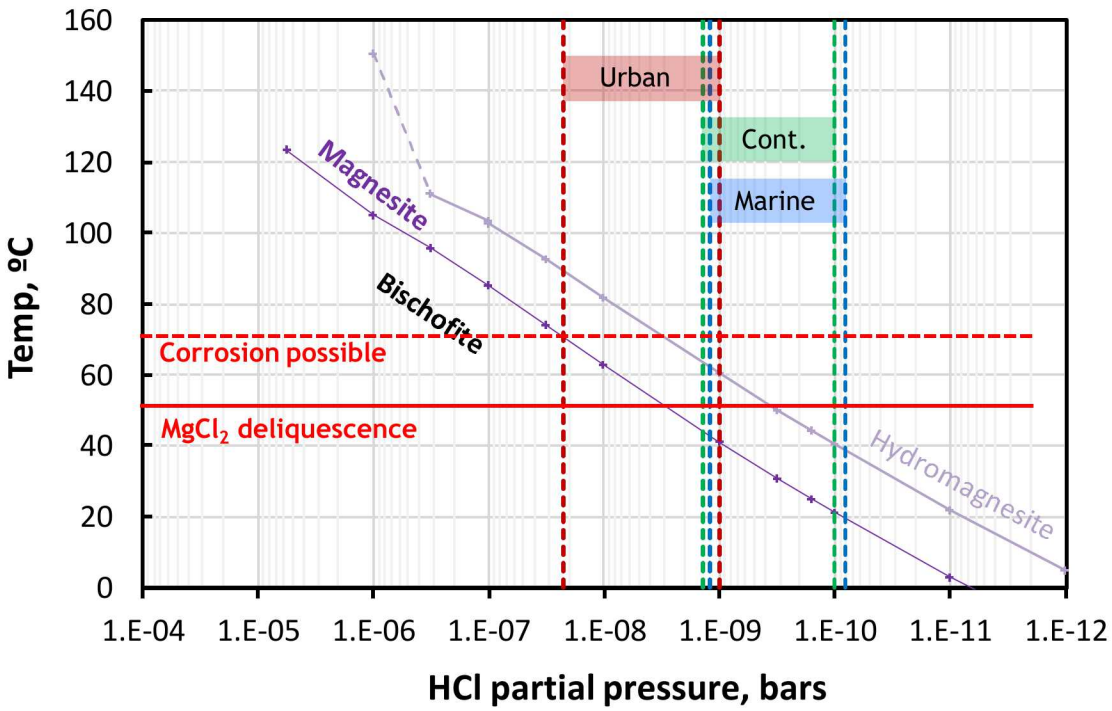

Experimental results:

$MgCl_2$ brine at 48°C, 40%RH, P_{HCL} = 0

- $MgCl_2$ brine, 48ºC, 40% RH, 2 L/min air flow.
- Partial conversion to carbonate observed; later chemical analysis suggests <10% chloride lost.
- Airflow was too low to support complete conversion. At 48ºC, one m^3 of air can only remove 1.3 – 13 µg chloride (hydromagnesite/magnesite). *Under field conditions, airflow is enormous.*

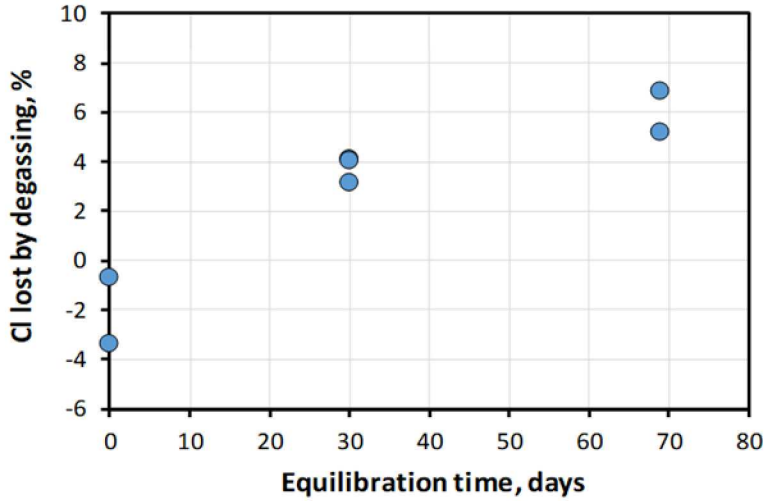

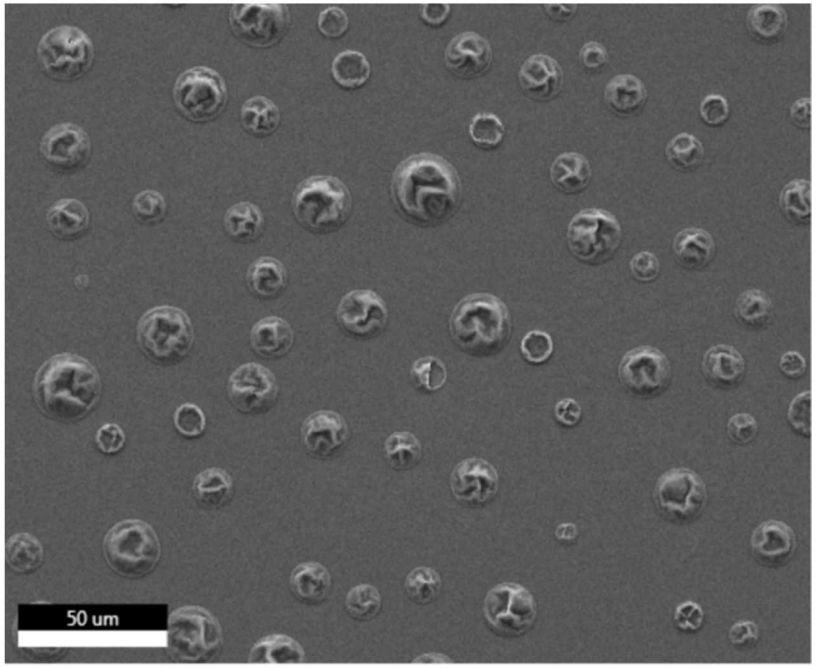

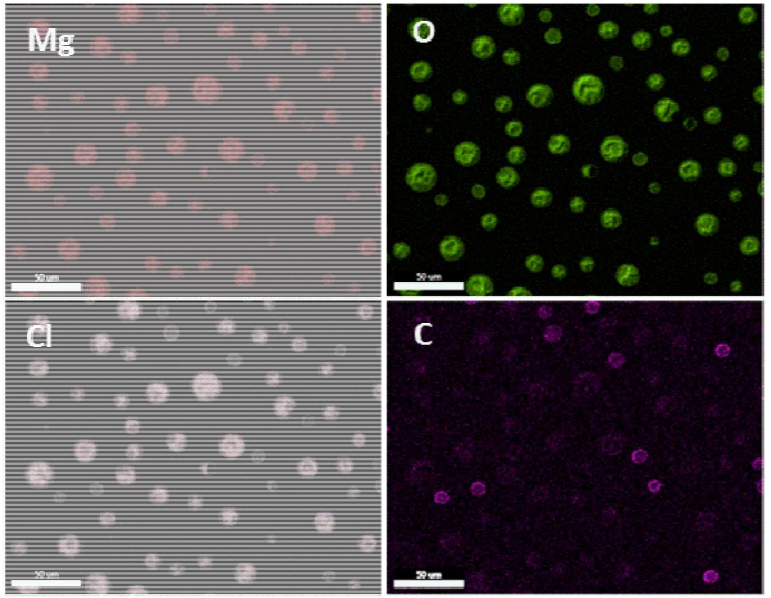

$MgCl_2$ Brine Stability

- $MgCl_2$ brine carbonation potentially results in brine dryout and loss of corrosive condition, if rate of degassing exceeds rate of salt aerosol accumulation.
- At low temperatures, rate of carbonation is limited by low HCl partial pressures generated by the brine.
- Under field conditions, $MgCl_2$ brine carbonation may be largely a function of ambient HCl partial pressures. Other acid gas reactions (e.g., H_2SO_4) may be more important in causing chloride loss.
- However, in laboratory settings, especially for "accelerated" (high temperature) conditions, brine dryout may be VERY important in limiting extent of corrosion.
- Additional $MgCl_2$ brine stability experiments in progress

Conclusions

- Atmospheric corrosion due to deposition and deliquescence of sea-salt aerosols is a frequently observed problem.
- Deliquescent brine composition/properties will control of extent of damage
  - Deliquescent brine compositions modeled by seawater evaporation; vary greatly with RH
    - Seawater at 98.6% RH
    - 6M NaCl (minor other components) at 74% RH
    - MgCl2 brine at the deliquescence point (25-36% RH).
  - Brine layer volume:
    - Controlled primarily by RH at the metal surface
    - Varies by orders of magnitude over the RH range of interest
    - Is unlikely to result in development of continuous brine films below 70% RH (for sea-salt aerosols deposited on sheltered surfaces).
  - Brine layer conductivity:
    - Varies with RH, peaking at about 75% RH (most concentrated NaCl brine)
    - Varies with temperature, for any given brine increasing by a factor of 3 to 5 as temperature increases from 10ºC to 80ºC.
- Atmospheric exchange reactions may have a pronounced effect on sea-salt brine stabilities
  - Dependence on temperature and ambient acid gas concentrations
  - May result in brine dryout, eliminating corrosive environment

References

Chen, Z. and Kelly, R. (2010). Computational modeling of bounding conditions for pit size on stainless steel in atmospheric environments. *Journal of the Electrochemical Society* **157**, C69-C78.

Chen, Z., Cui, F. and Kelly, R. (2008). Calculations of the cathodic current delivery capacity and stability of crevice corrosion under atmospheric environments. *Journal of the Electrochemical Society* **155**, C360-C368.

Clegg, S.L. and Brimblecombe, P., 1990, The solubility and activity coefficient of oxygen in salt solutions, *Geochimica Cosmochimica Acta,* 54, 3315-3328.

EPRI. (2014). *Calvert Cliffs Stainless Steel Dry Storage Canister Inspection.* Technical Report # 1025209. 460 p.

Harvie, C. E. and Weare, J. H. (1980). The prediction of mineral solubilities in natural waters: The Na-K-Mg-Ca-Cl-SO4-H2O system from zero to high concentration at 25 °C. *Geochimica et Cosmochimica Acta* **44**, 981-997.

Harvie, C. E., Weare, J. H., Hardie, L. A. and Eugster, H. P. (1980). Evaporation of seawater: calculated mineral sequences. *Science* **208**, pp. 498-500.

Harvie, C. E., Moller, N. and Weare, J. H. (1984). The prediction of mineral solubilities in natural waters: The Na-K-Mg-Ca-H-Cl-SO_4-OH-HCO_3-CO_3-CO_2-H_2O system to high ionic strengths at 25°C. *Geochimica et Cosmochimica Acta* **48**, pp. 723-751.

McCaffrey M., Lazar B., Holland H., "The evaporation path of seawater and the coprecipitation of Br^- and K^+ with halite," *Journal of Sedimentary Research* 57,5 (1987): pp. 928-937.

Pitzer, K. S. (1991). *Activity coefficients in electrolyte solutions. 2nd edition.* Boca Raton, FL: CRC Press.

Schindelholz, E. J., Moffat, H. K., Zavadil, K. R. and Sorensen, N. R. (2016). *Beyond Evans Drop: Electrolyte Evolution during Atmospheric Corrosion.* Sandia National Laboratories (SNL-NM), Albuquerque, NM (United States), p.

SNL. (2007). *In-drift Precipitates/Salts Model.* ANL-EBS-MD-000045 REV 03. Sandia National Laboratories, 358 p.

Van't Hoff, J. H. (1905). *Zur Bildung zeanischer Salzblagerungen: 1st issue*: Vieweg.

Van't Hoff, J. H. (1909). *Zur Bildung zeanischer Salzblagerungen: 2nd ed*: Vieweg.

Van't Hoff, J. H. (1912). *Untersuchungen tiber die Bildungsverhaltnisse der ozeanischen Salzablagerungen.* Leipzig: Akad. Verlags ges.

Wolery, T. W. and Jarek, R. L. (2003). *Software User's Manual, EQ3/6 Version 8.0.* Sandia National Laboratories, 376 p.